11th International Conference
on Advanced Materials

Rio de Janeiro Brazil
September 20 - 25

ICAM2009

Exciton dynamics in Silicon nanocrystals

L. Borrero(1)*, L. A. O. Nunes(1), M. R. B. Adreeta(1), Yu A. Pussep(1), J. Wojcik(2), P. Mascher(2), D. Comedi(3)
F. E. G. Guimarães(1)

(1) IFSC, Universidade de São Paulo, São Carlos, SP, Brazil, e-mail: lborrero@ursa.ifsc.usp.br
(2) CEDT, Dep. Eng. Phys., McMaster University, Hamilton, Ontario L8S 4L7, Canada
(3) LAFISO and CONICET, Dep. de Física, FACET, Universidad Nacional de Tucumán, Av. Independencia 1800, 4000 Tucumán, Argentina

Abstract – Silicon nanocrystals (Si-Ncs) embedded in a Silicon oxide matrix were studied by using photoluminescence (PL), Raman spectroscopy and time-resolved PL. Raman measurements demonstrate the coexistence of an amorphous and crystalline phases for Si-Ncs prepared at low annealing temperatures and smaller Si concentration. The effect of both phases on exciton dynamics, confinement and decay rates is evaluated by time resolved measurements.

The optical properties of Silicon nanocrystals (Si-Ncs) embedded in a Silicon oxide matrix have been studied by using photoluminescence (PL), Raman spectroscopy and time-resolved PL. Samples with different Silicon fractions ($0.36 \leq y \leq 0.42$) in Si_yO_{1-y} films were deposited on Quartz in an ECR-PECVD reactor and annealed at temperatures (T_a) varying from 900 °C to 1100 °C under Ar or (Ar+5%H_2) atmospheres. Infrared PL spectra were recorded and typical blue shift was observed for smaller nanocrystals. The luminescence is due to indirect recombination mediated by phonons of localized excitons in Si-Ncs. The first order Raman peak for Si-Ncs was asymmetrically broadened for all samples and downshifted by approximately 2 cm^{-1} when compared to the Raman signal of bulk Silicon single crystal. This result could be explained by a phonon confinement model inside the Si-Ncs. A large Raman band centered at about 480 cm^{-1} was also observed which accounts for amorphous Silicon (a-Si). The amorphous contribution increases with the decrease of the annealing temperature regarding the Si content constant. For a fixed annealing temperature, however, the crystalline component of the Raman spectra decreases together with the Si content in the Si_yO_{1-y}. This effect indicates that the density of Si-Ncs diminishes for small values of y. The exciton dynamics in Si-Ncs was analyzed by PL decay rates ($1/\tau$), which presented the well known exponential energy behavior consistent with a quantum confinement model. The PL time decay (τ) was measured for different emission energies and temperatures and can be well described by a stretched exponential law for all samples. We have measured $1/\tau$ for 4-300 K. When the emission energies vary from 1.4 to 1.8 eV, $1/\tau$ increases from 10^4 to 10^5 s^{-1}. However, $1/\tau$ values were higher (10^5-10^6 s^{-1}) for samples with higher amorphous component (smaller y and lowest T_a) and did not show appreciable energy dependence (Fig 1). In this case, excitons are no longer confined in the crystallite core and can reach nonradiative centers. We show that samples with smaller Si content exhibit larger volume fractions of amorphous Si and that passivation of the Si-Nc interface did not affect exciton confinement. At 1100 °C, the Ncs provides a better exciton confinement in Si crystalline core for all detection energies and sample temperature (Fig 2a). However, other non-radiative channels arises for large Si nanocrystals (low energies) for samples prepared at 1000 °C, indicating the lost of exciton confinement in the crystalline core (Fig 2b). In addition, we determine the exciton radiative rates dependence on energy and on sample temperature (Fig 3). This measurement allowed the determination of the exchange energy splitting between singlet and triplet states using the Brongersma et. al. model [APL, 76 (2000) 352] (Fig. 3 inset). This value increases from 2 to 8 meV for emission energies varying from 1.4 to 1.8 eV.

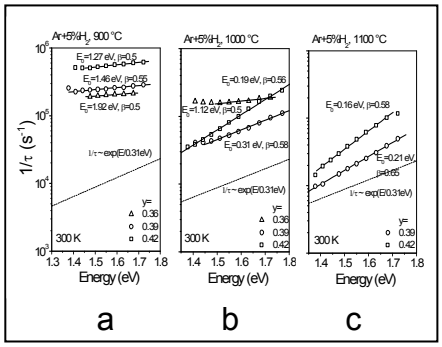

Figure 1: PL decay rate dependence on energy for samples annealed in Ar+5%H_2 at 900, 1000, 1100 °C.

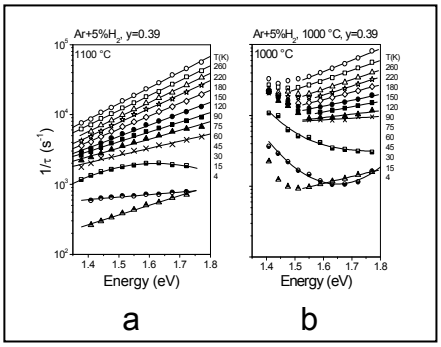

Figure 2: PL decay rate dependence on energy for sample (y=0.39) annealed in Ar+5%H_2 at (a) 1100 °C and (b) 1000 °C.

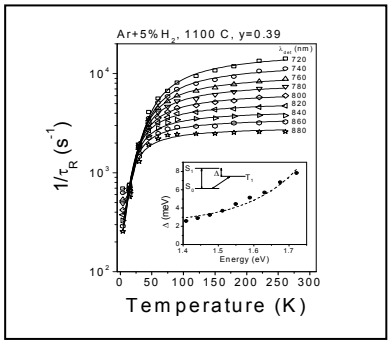

Figure 3: Radiative decay rate dependence on temperature for sample (y=0.39) annealed in Ar+5%H_2 at 1100 °C. Inset: exchange splitting.